学位論文

Calcium-dependent generation of *N*-acylethanolamines and lysophosphatidic acids by glycerophosphodiesterase GDE7

香川大学大学院医学系研究科
分子情報制御医学

Iffat Ara Sonia Rahman

Biochimica et Biophysica Acta 1861 (2016) 1881–1892

Contents lists available at ScienceDirect

Biochimica et Biophysica Acta

journal homepage: www.elsevier.com/locate/bbalip

Calcium-dependent generation of *N*-acylethanolamines and lysophosphatidic acids by glycerophosphodiesterase GDE7

Iffat Ara Sonia Rahman [a], Kazuhito Tsuboi [a], Zahir Hussain [a], Ryouhei Yamashita [b], Yoko Okamoto [b], Toru Uyama [a], Naoshi Yamazaki [b], Tamotsu Tanaka [b], Akira Tokumura [b,c], Natsuo Ueda [a,*]

[a] Department of Biochemistry, Kagawa University School of Medicine, 1750-1 Ikenobe, Miki, Kagawa 761-0793, Japan
[b] Institute of Biomedical Sciences, Tokushima University Graduate School, Tokushima 770-8505, Japan
[c] Department of Life Sciences, Faculty of Pharmacy, Yasuda Women's University, Hiroshima 731-0153, Japan

ARTICLE INFO

Article history:
Received 16 May 2016
Received in revised form 23 August 2016
Accepted 10 September 2016
Available online 13 September 2016

Keywords:
N-acylethanolamine
Glycerophosphodiesterase
Lysophosphatidic acid
Lysophospholipase D
Phospholipid

ABSTRACT

N-Acylethanolamines form a class of lipid mediators and include an endocannabinoid arachidonoylethanolamide (anandamide), analgesic and anti-inflammatory palmitoylethanolamide, and appetite-suppressing oleoylethanolamide. In animal tissues, *N*-acylethanolamines are synthesized from *N*-acylated ethanolamine phospholipids directly by *N*-acylphosphatidylethanolamine-hydrolyzing phospholipase D or through multi-step pathways via *N*-acylethanolamine lysophospholipids. We previously reported that glycerophosphodiesterase (GDE) 4, a member of the GDE family, has lysophospholipase D (lysoPLD) activity hydrolyzing *N*-acylethanolamine lysophospholipids to *N*-acylethanolamines. Recently, GDE7 was shown to have lysoPLD activity toward lysophosphatidylcholine to produce lysophosphatidic acid (LPA). Here, we examined the reactivity of GDE7 with *N*-acylethanolamine lysophospholipids as well as the requirement of divalent cations for its catalytic activity. When overexpressed in HEK293 cells, recombinant GDE7 proteins of human and mouse showed lysoPLD activity toward *N*-palmitoyl, *N*-oleoyl, and *N*-arachidonoyl-lysophosphatidylethanolamines and *N*-palmitoyl-lysoplasmenylethanolamine to generate their corresponding *N*-acylethanolamines and LPAs. However, GDE7 hardly hydrolyzed glycerophospho-*N*-palmitoylethanolamine. Overexpression of GDE7 in HEK293 cells increased endogenous levels of *N*-acylethanolamines and LPAs. Interestingly, GDE7 was stimulated by micromolar concentrations of Ca^{2+} but not by millimolar concentrations of Mg^{2+}, while GDE4 was stimulated by Mg^{2+} but was insensitive to Ca^{2+}. GDE7 was widely distributed in various tissues of humans and mice with the highest levels in their kidney tissues. These results suggested that GDE7 is a novel Ca^{2+}-dependent lysoPLD, which is involved in the generation of both *N*-acylethanolamines and LPAs.

1. Introduction

Fatty acyl ethanolamides, also denoted as *N*-acylethanolamines, comprise a series of endogenous lipid mediators and are ubiquitously present in various organisms, including mammals [1,2]. These molecules are involved in a variety of biological responses through specific receptors. Among different *N*-acylethanolamines, arachidonoylethanolamide (anandamide, *N*-arachidonoylethanolamine) was discovered as an endogenous agonist of cannabinoid receptors [3] and transient receptor potential vanilloid type-1 (TRPV-1) [4]. Palmitoylethanolamide (*N*-palmitoylethanolamine) mediates anti-inflammatory and analgesic actions through peroxisome proliferator-activated receptor-α (PPAR-α) [5,6]. Furthermore, oleoylethanolamide (*N*-oleoylethanolamine), an agonist of PPAR-α, TRPV-1, and GPR119, has appetite-suppressing and anti-obesity effects [5,7,8].

N-acylethanolamines are synthesized in cells on demand from membrane phospholipids. Phosphatidylethanolamine (PE) is *N*-acylated in the first reaction of this pathway by *N*-acyltransferase, forming *N*-acyl-PE (NAPE) [9,10]. The second step is the direct release of *N*-acylethanolamine from NAPE by NAPE-hydrolyzing phospholipase D (NAPE-PLD) [11] (Fig. 1A). In addition, *N*-acylethanolamine can be formed from NAPE in alternative multistep pathways via *N*-acyl-lysoPE [12,13]. Alkenylacyl-glycerophosphoethanolamine (plasmenylethanolamine, PlsEt) is another class of ethanolamine phospholipids, and *N*-acyl-PlsEt exists in brain [13,14]. *N*-acylethanolamine is also formed from *N*-acyl-PlsEt through both NAPE-PLD-dependent and -independent pathways (Fig. 1B) [13]. Glycerophosphodiesterase (GDE) 1 was considered to be a constituent of NAPE-PLD-independent pathway because this enzyme generated *N*-acylethanolamine from glycerophospho-*N*-acylethanolamine, an intermediate metabolite in this pathway (Fig. 1A) [15]. We also found that GDE1 has a relatively low lysophospholipase D (lysoPLD) activity forming *N*-acylethanolamine

* Corresponding author.
E-mail address: nueda@med.kagawa-u.ac.jp (N. Ueda).

http://dx.doi.org/10.1016/j.bbalip.2016.09.008
1388-1981/

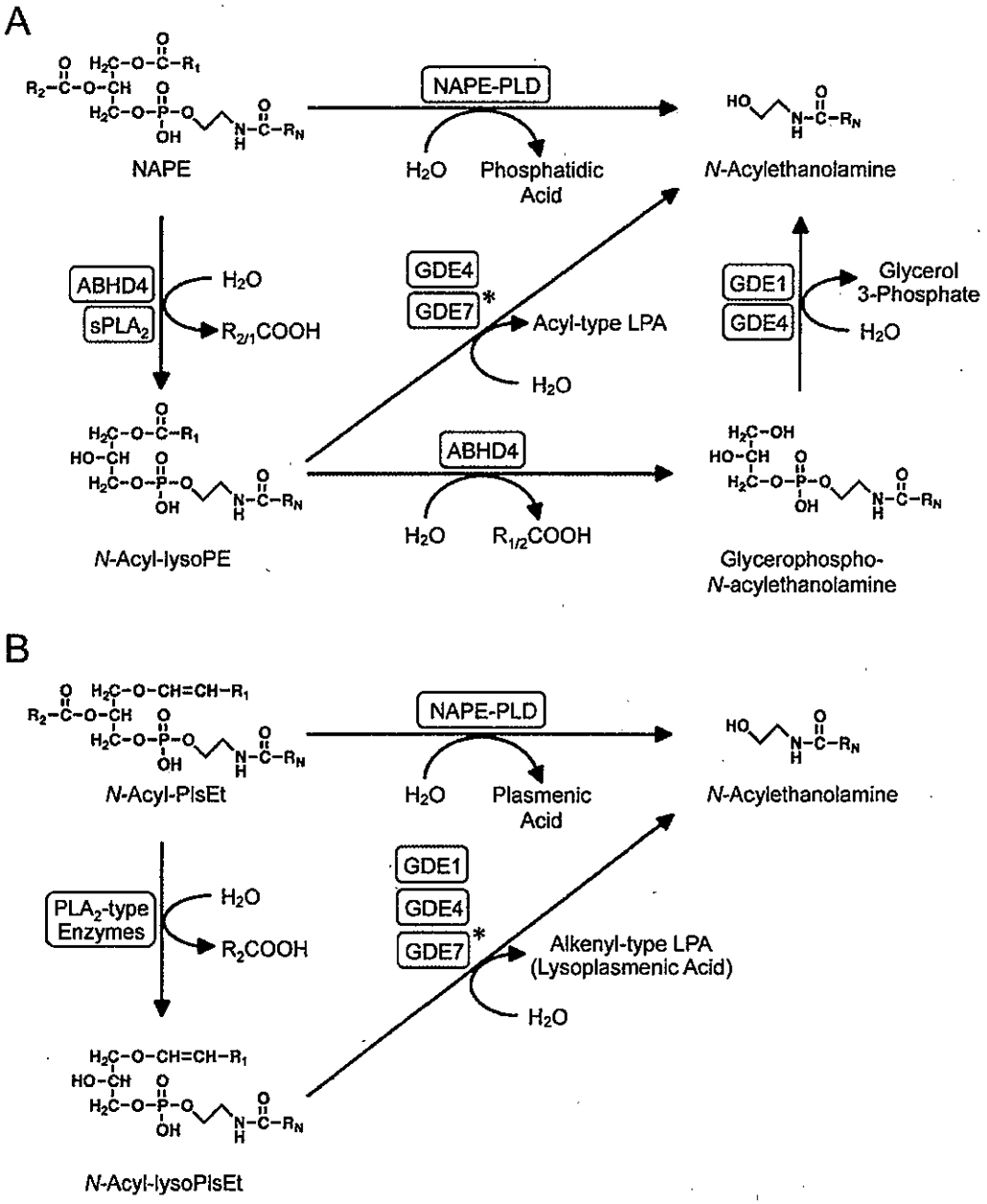

Fig. 1. Biosynthetic pathways of *N*-acylethanolamine from NAPE (A) and *N*-acyl-PlsEt (B). *, GDE7 was shown to catalyze the indicated reactions for the first time in the present study. ABHD4, α/β-hydrolase domain-containing protein 4; $sPLA_2$, secretory phospholipase A_2.

from *N*-acyl-lysoPlsEt [13]. Moreover, we recently reported that GDE4, another member of the GDE family, also shows lysoPLD activity and produces *N*-acylethanolamine from both *N*-acyl-lysoPlsEt and *N*-acyl-lysoPE [16]. The results showed a possibility that GDE4 is also involved in the NAPE-PLD-independent *N*-acylethanolamine formation.

Very recently, Ohshima et al. reported that GDE7 is the closest protein to GDE4 among seven members of the mammalian GDE family and that GDE7 as well as GDE4 has lysoPLD activity toward lysophosphatidylcholine (lysoPC), producing lysophosphatidic acid (LPA) [17]. Thus, we were interested whether GDE7 contributes to the *N*-acylethanolamine biosynthesis by its lysoPLD activity. In the present study, we compared the catalytic properties of recombinant proteins of human GDE7 (hGDE7), mouse GDE7 (mGDE7), human GDE4 (hGDE4), and mouse GDE4 (mGDE4). The results showed that hGDE7 and mGDE7 function as lysoPLDs which hydrolyze *N*-acyl-lysoPE and *N*-acyl-lysoPlsEt to yield *N*-acylethanolamine. Moreover, we revealed for the first time that the generation of *N*-acylethanolamine and LPA by GDE7 is dependent on Ca^{2+}.

2. Materials and methods

2.1. Materials

[1-^{14}C]Palmitic acid, 1,2-[1′-^{14}C]dipalmitoyl-*sn*-glycero-3-phosphocholine (1,2-[^{14}C]dipalmitoyl-phosphatidylcholine (1,2-[^{14}C]dipalmitoyl-PC)), and 1-[1′-^{14}C]palmitoyl-2-hydroxy-*sn*-glycero-3-phosphocholine (1-[^{14}C]palmitoyl-lysoPC) were purchased from PerkinElmer Life Science (Boston, MA, USA); [1-^{14}C]oleic and [1-^{14}C]arachidonic acids were from Moravek Biochemicals (Brea, CA, USA); horseradish peroxidase-linked anti-mouse IgG antibody was

from GE Healthcare (Piscataway, NJ, USA); arachidonic acid was from Nu-Chek Prep (Elysian, MN, USA); palmitic and oleic acids, 1,2-dioleoyl-*sn*-glycero-3-phosphoethanolamine (1,2-dioleoyl-PE), 1-palmitoyl-lysoPC, and anti-FLAG M2 monoclonal antibody were from Sigma-Aldrich (St. Louis, MO, USA); 1-*O*-1′-(*Z*)-octadecenyl-2-oleoyl-*sn*-glycero-3-phosphoethanolamine (1-octadecenyl-2-oleoyl-PlsEt) and 1-heptadecanoyl-2-hydroxy-*sn*-glycerol-3-phosphate (1-heptadecanoyl-LPA) were from Avanti Polar Lipids (Alabaster, AL, USA); *N*-(2-hydroxyethyl)-hexadecanamide-7,7,8,8-d_4 (deuterated palmitoylethanolamide) and URB597 were from Cayman Chemical (Ann Arbor, MI, USA); sodium orthovanadate, dithiothreitol (DTT), 3(2)-*t*-butyl-4-hydroxyanisole (BHA), Triton X-100, and Tween 20 were from Wako Pure Chemical (Osaka, Japan); protein assay dye reagent concentrate was from Bio-Rad (Hercules, CA, USA); pDsRed2-ER vector and human MTC Multiple Tissue cDNA Panels were from Clontech/Takara Bio (Mountain View, CA, USA); Ex Taq polymerase and random hexamer were from Takara Bio (Ohtsu, Japan); precoated silica gel 60 F_{254} aluminum sheets for thin-layer chromatography (TLC) (20 × 20 cm, 0.2-mm thickness) and Immobilon-P were from Merck Millipore (Darmstadt, Germany); Dulbecco's modified Eagle's medium (DMEM), non-essential amino acid solution, Lipofectamine 2000, TRIzol, Moloney murine leukemia virus reverse transcriptase, Alexa 488-conjugated anti-mouse IgG antibody, and the expression vectors, pcDNA3.1(+), pcDNA3.1/Hygro(−), pcDNA3.1/Hygro(+), and pCR3.1, were from Invitrogen/Thermo Fisher Scientific (Carlsbad, CA, USA); fetal calf serum (FCS) was from Biowest (Nuaillé, France); Pierce Western Blotting Substrate Plus was from Thermo Fisher Scientific (Waltham, MA, USA); normal goat serum was from Vector Laboratories (Burlingame, CA, USA); 4% Paraformaldehyde Fixative solution was from Muto Pure Chemicals (Tokyo, Japan); Permafluor was from Immunotech (Marseille, France); human embryonic kidney 293 (HEK293) cells were from Health Science Research Resources Bank (Osaka, Japan).

2.2. Syntheses of radioactive molecules

1,2-Dioleoyl-*sn*-glycero-3-phospho(*N*-[^{14}C]acyl)ethanolamines (*N*-[^{14}C]acyl-1,2-dioleoyl-PEs) were prepared by allowing their corresponding 1-^{14}C-labeled fatty acids to react with 1,2-dioleoyl-PE according to the method of Schmid et al. [18]. 1-*O*-1′-(*Z*)-Octadecenyl-2-oleoyl-*sn*-glycero-3-phospho(*N*-[^{14}C]palmitoyl)ethanolamine (*N*-[^{14}C]palmitoyl-1-octadecenyl-2-oleoyl-PlsEt) was also synthesized from [1-^{14}C]palmitic acid and 1-octadecenyl-2-oleoyl-PlsEt by the same method. 1-Oleoyl-2-hydroxy-*sn*-glycero-3-phospho(*N*-[^{14}C]acyl) ethanolamines (*N*-[^{14}C]acyl-1-oleoyl-lysoPEs) and 1-*O*-1′-(*Z*)-octadecenyl-2-hydroxy-*sn*-glycero-3-phospho(*N*-[^{14}C]palmitoyl) ethanolamine (*N*-[^{14}C]palmitoyl-1-octadecenyl-lysoPlsEt) were prepared from their corresponding *N*-[^{14}C]acyl-PEs and *N*-[^{14}C]palmitoyl-1-octadecenyl-2-oleoyl-PlsEt, respectively, with group IB secretory phospholipase A_2 purified from rat stomach as described previously [19]. *sn*-Glycero-3-phospho(*N*-[^{14}C]palmitoyl)ethanolamine (glycerophospho-*N*-[^{14}C]palmitoylethanolamine ([^{14}C]GP-NPE)) was prepared from *N*-[^{14}C]palmitoyl-1,2-dioleoyl-PE by alkaline hydrolysis and recovered in the organic layer by the method of Bligh and Dyer [20] after neutralization of the reaction mixture. The synthesized radioactive molecules were purified by TLC prior to use.

2.3. Constructions of expression vectors

The cDNAs encoding C-terminally FLAG-tagged mGDE4 and mGDE7 were generated by RT-PCR. Construction of a pcDNA3.1(+) expression vector harboring cDNA for C-terminally FLAG-tagged mGDE4 was described previously [16]. For mGDE7, total RNA was isolated with TRIzol reagent from the kidney of mouse (C57BL/6, Japan SLC), and cDNA was then prepared by using Moloney murine leukemia virus reverse transcriptase and random hexamer. We next prepared two cDNA fragments of mGDE7 by PCR using this cDNA as a template. The 5′-portion of mouse GDE7 cDNA was amplified with the forward primer 5′-CGAA GCTTGGCGCCATGATCCCTCTCCTGTACT-3′ and the reverse primer 5′-GAAGGCCACTTCAAAATCCG-3′, and its digestion with *Hin*dIII and *Pst*I gave a 0.54-kb fragment. The 3′-portion was amplified with the forward primer 5′-GACCGGAATGAGATTACTATTTGGG-3′ and the reverse primer 5′-ATCTCGAGCTACTTATCGTCGTCATCCTTGTAATCTGCGGCTTTTTTAAG AGAAAGACAGGACAGGGC-3′, and its digestion with *Pst*I and *Xho*I gave a 0.49-kb fragment. These primers were designed according to the cDNA sequence (Genbank™ accession number NM_024228.2). The two fragments were sequentially inserted between *Hin*dIII and *Xho*I sites of pCR3.1 vector. The obtained full-length cDNA for C-terminally FLAG-tagged mGDE7 was finally subcloned into an expression vector pcDNA3.1(+) at the same sites. The cDNAs encoding C-terminally FLAG-tagged hGDE4 and hGDE7 were synthesized by Takara Bio according to the reported sequences (EU192951.1 and NM_024307.2, respectively). The sequence for the FLAG-tagged hGDE4 consisted of 5′-gcgccaacaGGTACC, the coding region of EU192951.1 without the stop codon, and ggatccgactacaaggatgacgatgacaagtagtaaTCTAGActgcgcc-3′ (uppercase letters show the restriction sites). The synthesized DNA was digested with *Kpn*I and *Xba*I, and inserted into the corresponding sites of an expression vector pcDNA3.1/Hygro(+). The sequence for the FLAG-tagged hGDE7 consisted of 5′-gcgccaacaCTCGAGgcc, the coding region of NM_024307.2 without the stop codon, and ggatccgactacaaggatgacgatgacaagtagtAAGCTTactgcgcc-3′. The synthesized DNA was digested with *Xho*I and *Hin*dIII, and inserted into the corresponding sites of pcDNA3.1/Hygro(−). The inserted cDNAs were sequenced in both directions using an Applied Biosystems 3130 Genetic Analyzer (Thermo Fisher Scientific).

2.4. Immunocytochemistry

HEK293 cells were cultured at 37 °C on poly-L-lysine-coated 18-mm glass coverslips in DMEM containing 10% FCS and 0.1 mM non-essential amino acids in a humidified 5% CO_2 and 95% air incubator. The cells were then transfected with both of pDsRed2-ER vector (1 μg) and the expression vector harboring cDNA for GDE7 or GDE4 (1 μg) by using 6 μl of Lipofectamine 2000 according to the manufacturer's instruction. After 24 h, the cells were fixed with 4% paraformaldehyde in 0.1 M phosphate-buffered saline (PBS) (pH 7.4) for 15 min. The fixed cells were rinsed in PBS twice and permeabilized with 0.2% (w/v) Triton X-100 in PBS for 15 min. After blocking with 10% normal goat serum in PBS for 1 h, the cells were incubated with anti-FLAG antibody (1:500 dilution) in 1% normal goat serum/PBS for 1 h at room temperature. The cells were washed with PBS twice and labeled with Alexa 488-conjugated anti-mouse IgG antibody (1:1000 dilution) in 1% normal goat serum/PBS for 1 h. The specimen coverslips were mounted on glass slides using Permafluor, a mounting medium, and were observed with an LSM 700 confocal laser microscope (Carl Zeiss, Germany).

2.5. Expressions of recombinant GDE7 and GDE4

HEK293 cells were cultured to 70% confluency in a poly-L-lysine-coated 100-mm dish containing DMEM with 10% FCS and 0.1 mM non-essential amino acids. The cells were then transfected with 16 μg of the expression vector harboring cDNA for GDE7 or GDE4 by using 40 μl of Lipofectamine 2000. Control cells were also prepared by transfection with the insert-free pcDNA3.1/Hygro(−) vector. For liquid chromatography-tandem mass spectrometry (LC-MS/MS) analyses, the medium was changed to FCS-free DMEM at 24 h after the transfection. The cells were further cultured for 24 h, harvested by scraping, and subjected to lipid extraction. For enzyme assays, the cells were harvested by scraping at 48 h after the transfection and sonicated three times each for 3 s in 50 mM Tris–HCl (pH 7.4). The cell homogenates were then centrifuged at 105,000 ×*g* for 55 min. The resultant pellets were

suspended in 20 mM Tris–HCl (pH 7.4) and used as membrane fractions.

2.6. Preparations of tissue homogenates

Male C57BL/6 mice (8 weeks old, Japan SLC) were anesthetized by intraperitoneal injection of pentobarbital and sacrificed by decapitation. The brains and kidneys were isolated, cut into small pieces, and homogenized in 9 times the volume (v/w) of ice-cold 20 mM Tris–HCl (pH 7.4)/0.32 M sucrose with a Polytron homogenizer. The homogenates were centrifuged at 800 ×*g* for 15 min, and the resultant supernatants were used as "homogenates". The protein concentration was determined by the method of Bradford [21] with bovine serum albumin as a standard.

2.7. Western blotting

Protein samples were denatured in 20 mM Tris–HCl (pH 6.8) containing 1% SDS, 4 M urea, 5% 2-mercaptoethanol, and 0.005% bromophenol blue at 60 °C for 10 min, separated by SDS-PAGE on a 12% gel, and electrotransferred to a hydrophobic polyvinylidene difluoride membrane (Immobilon-P). The following procedures were performed at room temperature. The membrane was blocked with PBS containing 5% non-fat dried milk and 0.1% Tween 20 for 1 h and then incubated with anti-FLAG antibody (1:4000 dilution) in the blocking buffer for 1 h, followed by incubation with horseradish peroxidase-linked anti-mouse IgG antibody (1:10,000 dilution) in the blocking buffer for 1 h. After the treatment with Pierce Western Blotting Substrate Plus, FLAG-tagged proteins were visualized and their intensities were quantified with an ImageQuant LAS 4010 lumino-imaging analyzer (GE Healthcare). Their expression levels were then estimated by using a standard curve drawn with different amounts (1–30 μg of protein) of the membrane fraction from the hGDE7-expressing cells. The enzyme activities were normalized to the respective expression levels and expressed as relative values (shown in parentheses, Fig. 4E).

2.8. Enzyme assays

Unless otherwise mentioned, the enzyme samples were incubated with 25 μM *N*-[^{14}C]palmitoyl-lysoPE (25,000 cpm, dissolved in 5 μl of ethanol) at 37 °C for 30 min in 100 μl of 50 mM Tris–HCl (pH 7.4) containing 3 mM DTT, 3 μM URB597, and either 2 mM $CaCl_2$ (for GDE7) or 2 mM $MgCl_2$ (for GDE4). URB597 was used to inhibit fatty acid amide hydrolase, an enzyme degrading *N*-acylethanolamines [22,23]. The reactions were terminated by the addition of 0.32 ml of a mixture of chloroform/methanol (2:1, v/v) containing 5 mM BHA. After centrifugation, 100 μl of the organic phase was spotted on a silica gel thin-layer plate (10-cm height), and TLC was developed at 4 °C for 20 min with a mixture of chloroform/methanol/acetic acid (90:10:5, v/v). For the assays in Fig. 5, 25 μM of *N*-[^{14}C]palmitoyl-PE, *N*-[^{14}C]oleoyl-lysoPE, *N*-[^{14}C]arachidonoyl-lysoPE, and *N*-[^{14}C]palmitoyl-lysoPlsEt (25,000 cpm, dissolved in 5 μl of ethanol) were also used as radioactive substrates in the same reaction mixture.

For the assay of glycerophospho-*N*-acylethanolamine-hydrolyzing activity (Fig. 5), the enzyme samples were incubated with 25 μM [^{14}C]GP-NPE (25,000 cpm, dissolved in 5 μl of ethanol) under the same assay conditions [13,16]. The reactions were terminated by the addition of 0.32 ml of a mixture of chloroform/methanol/1 M citric acid (8:4:1, v/v) containing 5 mM BHA. The organic phase was subjected to TLC at 4 °C for 20 min with a mixture of chloroform/methanol/28% ammonium hydroxide (80:20:2, v/v).

For the assay of lysoPC-hydrolyzing activity (Figs. 5 and 6E), the enzyme samples were incubated with 25 μM of 1-[^{14}C]palmitoyl-lysoPC (25,000 or 10,000 cpm, dissolved in 5 μl of ethanol) under the same assay conditions except that the phosphatase inhibitor sodium orthovanadate at 100 μM, instead of URB597, was added [16] to protect the produced [^{14}C]LPA from degradation [24]. The reactions were terminated by the addition of 0.32 ml of a mixture of chloroform/methanol/1 M citric acid (8:4:1, v/v) containing 5 mM BHA. TLC was developed at 4 °C for 25 min with a mixture of chloroform/methanol/formic acid/water (60:30:7:3, v/v).

After TLC development, the radioactivities of the substrates and products on the plate were quantified by a FLA7000 image analyzer (FUJIFILM, Tokyo, Japan). The enzyme activity was then calculated based on both the radioactivities. Since the recovery rate of [^{14}C]GP-NPE in the organic layer was as low as around 50%, the radioactivities of this substrate were normalized by multiplying the measured values by 2. All the enzyme assays were performed in triplicate.

2.9. Lipid analyses by LC-MS/MS

Lipids were extracted from cells by the modified method of Bligh and Dyer, essentially as described previously [25]. In this method, cells were suspended in 3.8 ml of a mixture of chloroform/methanol/0.05 M KCl (1:2:0.8, v/v) on ice followed by sonication for 10–20 s. Internal standards were then added to this suspension. After standing for 20 min on ice, the mixture was centrifuged at 1200 ×*g* for 10 min. The supernatant was withdrawn, and the resultant pellet was mixed with 1.9 ml of chloroform/methanol/water (1:2:0.8) followed by centrifugation. The supernatants were combined, and 1.5 ml each of chloroform and water were added to the sample to produce phase separation. After centrifugation of the mixture, the organic lower phase was withdrawn. The upper layer was mixed with 3 ml of chloroform/methanol (17:3), and the mixture was centrifuged. The solvent of the combined lower layers was evaporated under a stream of nitrogen gas, and the obtained lipid extract (Extract A) was reconstituted in 0.1 ml of methanol/water (95:5) containing 0.05 M ammonium formate (Solvent A) in a glass insert set in a brown glass vial for LC-MS/MS for *N*-acylethanolamines. The remaining aqueous layer was acidified to pH 2.0–2.5 with 1 M HCl, and 3 ml of chloroform/methanol (17:3) mixture was added, followed by centrifugation. A large portion of LPA was recovered into the resultant organic layer. This procedure was repeated. Thus obtained lipid extract (Extract B) was dried down in a glass insert set in a brown vial under a stream of nitrogen gas, and reconstituted in 0.1 ml of Solvent A for quantification of LPAs.

LC-MS/MS was performed on a quadrupole-linear ion trap hybrid mass spectrometry system, 4000 Q TRAP (Applied Biosystems/MDS Sciex, Concord, Ontario, Canada) with a 1100 liquid chromatography system (Agilent Technologies, Wilmington, DE, USA) combined with an HTS-PAL autosampler (CTC Analytics AG, Zwingen, Switzerland), as described previously [13,16]. *N*-acylethanolamine species in Extract A were analyzed by liquid chromatography on a Supelco Ascentis Express C18 reverse phase column (100 mm × 2.1 mm, 2.7-μm particle size) with Solvent A at a flow rate of 0.15 ml/min. LPA species in Extract B were separated by the use of a Tosoh TSK-ODS-100Z column (150 mm × 2 mm, 5-μm particle size) with Solvent A at a flow rate of 0.20 ml/min. Routinely, 5-μl aliquots of the test solutions in an insert were applied using the autosampler. The positive ion mode of operation with multiple reaction monitoring was used for *N*-acylethanolamine species. Q1 was set to the protonated molecular ion as the precursor ion, and $[ethanolamine]^+$ at *m/z* 62 was selected as the fragment ion for Q3. The negative ion mode of operation with multiple reaction monitoring was used for LPA species, and $[deprotonated\ cyclic\ glycerophosphate]^-$ at *m/z* 153 was selected for Q3 in combination with the deprotonated molecular ion as Q1. The molecular species of *N*-acylethanolamine and LPA were quantified using deuterated palmitoylethanolamide and 1-heptadecanoyl-LPA as internal standards, respectively. Values were represented as pmol/mg of protein.

2.10. RT-PCR

Total RNAs were isolated with TRIzol reagent from various tissues of C57BL/6 mice (male, 8 weeks old, Japan SLC). cDNAs were then

prepared from 5 μg of total RNA by using Moloney murine leukemia virus reverse transcriptase and random hexamer, and were subjected to PCR amplification by Ex Taq DNA polymerase. To examine distribution in human tissues, human MTC Multiple Tissue cDNA Panels I and II were used as templates for PCR amplification. The forward and reverse primers were as follows: for mGDE7, 5′-CCTGTCCCGCCAGTCAGGCCTA AATAAGG-3′ and 5′-GCCCCAGGTAGTAGAGCAGCAGTATCCAG-3′ (nucleotides 324–352 and 672–700, respectively, in GenBank™ accession number NM_024228.2); hGDE7, 5′-CCTGTGCCGCCAGTCGGGCCTAAACA GGG-3′ and 5′-GCCCCAGGTAGTAGGAAAGCAGCACCCAG-3′ (nucleotides 346–374 and 694–722, respectively, in NM_024307.2); hGDE4, 5′-CAGC GATTCCTCAGTAAACACATCTCTCAC-3′ and 5′-GGTTCTTTTAGCTTCAGTAT AATAGAAGGC-3′ (nucleotides 249–278 and 836–865, respectively, in NM_182569.3). The PCR conditions used were as follows: for mGDE7, denaturation at 94 °C for 48 s, annealing at 66 °C for 48 s, and extension at 72 °C for 48 s (30 cycles); for hGDE7, denaturation at 94 °C for 48 s, annealing at 51 °C for 48 s, and extension at 72 °C for 48 s (30 cycles); for hGDE4, denaturation at 94 °C for 48 s, annealing at 54 °C for 48 s, and extension at 72 °C for 48 s (33 cycles). PCRs for glyceraldehyde-3-phosphate dehydrogenase (GAPDH), a housekeeping gene, of humans [26] and mice [11] were performed as described previously. PCR products were electrophoresed on agarose gels and stained with ethidium bromide. PCR analyses of human tissue cDNA panels were repeated three times, and RT-PCR analyses of mouse tissue RNAs were performed three times with different animals. Similar results were obtained from each analysis, and representative results were shown in Fig. 8.

3. Results

3.1. Functional expressions of GDE7 and GDE4

Fig. 2 shows the alignment of the deduced amino acid sequences of hGDE7, mGDE7, hGDE4, and mGDE4. The estimated molecular masses were 36.6, 38.5, 36.2, and 35.9 kDa, respectively. The identities of the deduced amino acid sequences between GDE7 and GDE4 were 42.2% (human) and 40.3% (mouse). The identity between hGDE7 and mGDE7 was 77.6%. These proteins were predicted to contain two transmembrane domains. We prepared cDNAs encoding these four proteins tagged with a FLAG sequence at C-termini and transiently expressed these FLAG-tagged proteins in HEK293 cells as described in Materials and Methods. To examine the intracellular distribution, the cells were immunostained with anti-FLAG antibody and observed with a confocal laser-scanning microscope. As for hGDE7, punctate signals were observed throughout the cytoplasm (Fig. 3A). Co-introduction of DsRed2-ER, a fluorescent protein targeted to endoplasmic reticulum (ER) with the aid of the ER targeting sequence of calreticulin and the ER retention sequence (KDEL), revealed that the GDE7 signals partially colocalized with this ER marker. On the other hand, most of the signals for hGDE4 colocalized with DsRed2-ER, suggesting its predominant localization in ER (Fig. 3B). We also observed that the distributions of mGDE7 and mGDE4 are similar to those of hGDE7 and hGDE4, respectively (data not shown). These results were in good agreement with the previous observations for hGDE4 [27], mGDE7 [17], and mGDE4 [17].

We next allowed the membrane fractions to react with *N*-[^{14}C] palmitoyl-lysoPE and separated the radioactive product from the remaining substrate by TLC. Western blotting with anti-FLAG antibody confirmed the expressions of each recombinant protein (Fig. 4A and B). Since we found that the enzyme activities of GDE7 and GDE4 were stimulated by $CaCl_2$ and $MgCl_2$, respectively (details shown in Fig. 6A and B), either of these divalent cations was added to the reaction mixtures at 2 mM for the optimal conditions. The membrane fractions of the cells expressing mGDE4 produced the radioactive band corresponding to [^{14}C]palmitoylethanolamide (Fig. 4D), which is in agreement with our previous result [16]. The activity was estimated to be 3.8 nmol/min/mg of protein (Fig. 4E). Similarly, the membrane fractions

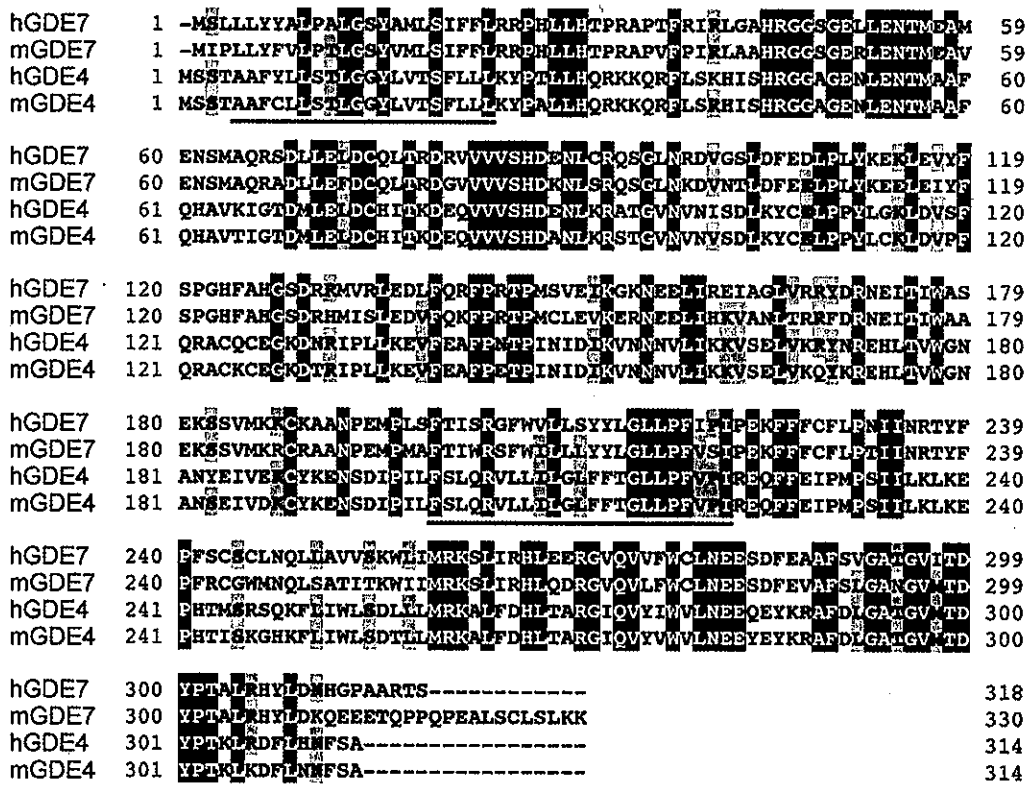

Fig. 2. Deduced amino acid sequences of hGDE7, mGDE7, hGDE4, and mGDE4. The sequences are aligned using the program GENETYX-MAC (version 17). Closed and shaded boxes indicate identity in all four and any three polypeptides, respectively. Underlines denote putative transmembrane domains common to the four proteins predicted by TMHMM 2.0 program [44].

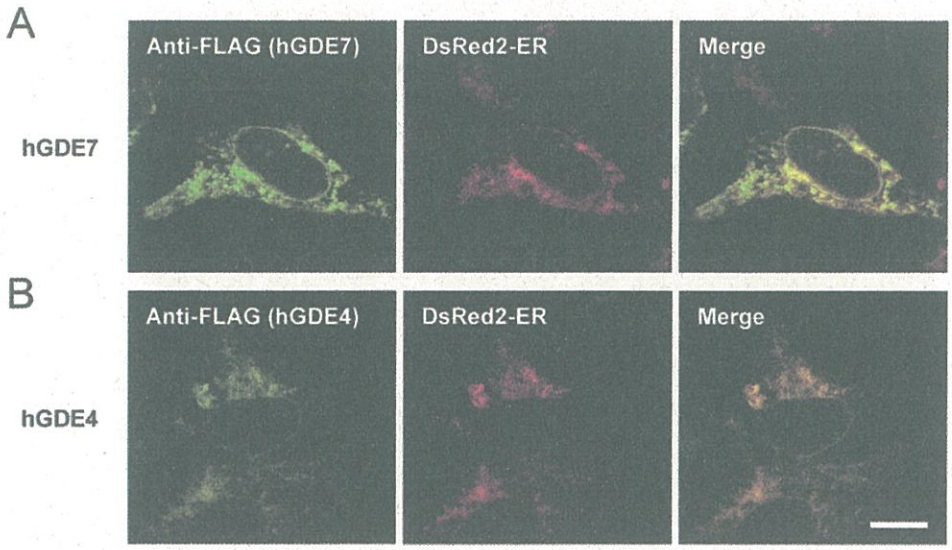

Fig. 3. Intracellular localization of GDE7 and GDE4. HEK293 cells were transfected with the expression vectors for DsRed2-ER and either FLAG-tagged hGDE7 (A) or hGDE4 (B). The cells were then immunostained with anti-FLAG antibody and observed with a confocal laser-scanning microscope. Signals for FLAG-tagged enzymes (hGDE7 and hGDE4) and DsRed2-ER are shown in green and red, respectively. The overlap of both signals is shown in yellow (Merged). Scale bar, 10 μm.

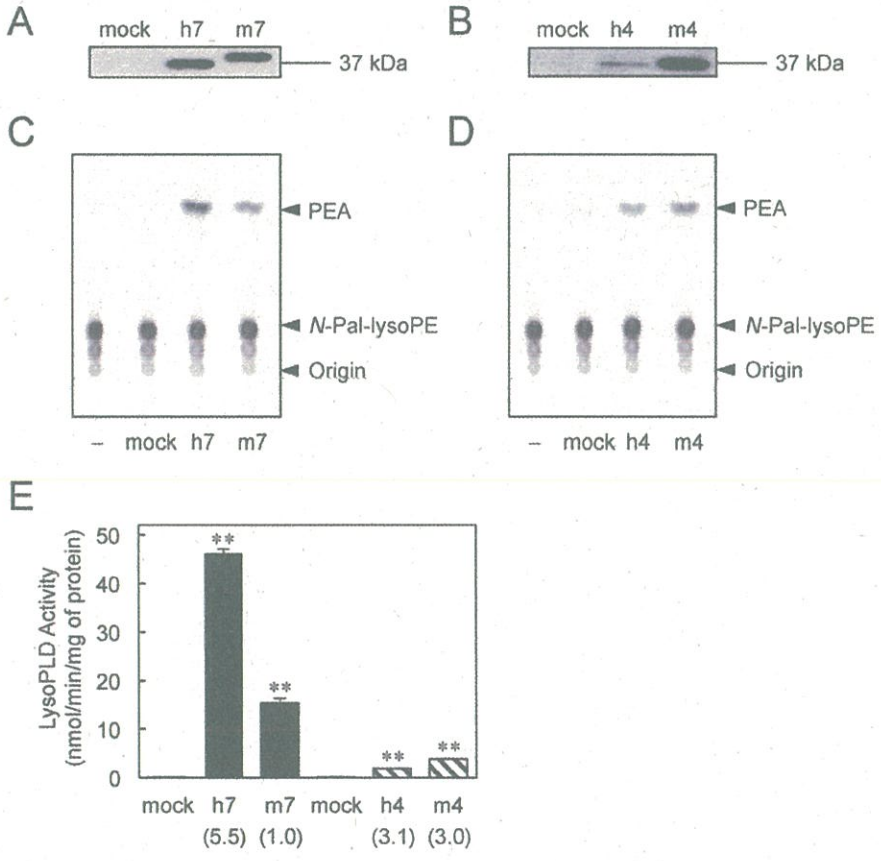

Fig. 4. LysoPLD activities of hGDE7 (h7), mGDE7 (m7), hGDE4 (h4), and mGDE4 (m4) toward *N*-[^{14}C]palmitoyl-lysoPE. HEK293 cells were transfected with the insert-free vector (mock) or the expression vector harboring cDNA for one of the four FLAG-tagged enzymes. (A and B) the membrane fractions (10 and 20 μg of protein in A and B, respectively) were analyzed by Western blotting with anti-FLAG antibody. (C–E) the membrane fractions (0.6 and 2 μg of protein in C and D, respectively) were allowed to react with 25 μM of *N*-[^{14}C]palmitoyl-lysoPE in the presence of either 2 mM $CaCl_2$ (C) or 2 mM $MgCl_2$ (D). The produced [^{14}C]palmitoylethanolamide was separated by TLC (C and D) and quantified. The calculated lysoPLD activities are expressed per one milligram of total proteins in the membrane fractions (a bar graph in E, mean values ± S.D., $n = 3$). The activities normalized to the respective expression levels are also expressed as relative values (parentheses in E). Arrowheads indicate the positions of the origin and authentic compounds on the TLC plates. *N*-Pal-lysoPE, *N*-palmitoyl-lysoPE; PEA, palmitoylethanolamide. **, $P < 0.01$ compared with mock (ANOVA followed by Dunnett's test).

of the cells expressing hGDE7 and mGDE7 as well as hGDE4 hydrolyzed *N*-[^{14}C]palmitoyl-lysoPE to [^{14}C]palmitoylethanolamide at the rates of 46, 15, and 1.9 nmol/min/mg of protein, respectively (Fig. 4C–E). In contrast, the membrane fraction of the control cells produced only a trace amount of [^{14}C]palmitoylethanolamide (<0.14 nmol/min/mg of protein). Since the expression levels of the FLAG-tagged proteins were different from each other (Fig. 4A and B), the activities were normalized to the respective expression levels. The relative values for hGDE7, mGDE7, hGDE4, and mGDE4 were estimated to be 5.5, 1.0, 3.1, and 3.0, respectively (the parentheses in Fig. 4E). These results showed that GDE7 as well as GDE4 can hydrolyze *N*-acyl-lysoPEs to *N*-acylethanolamines by using lysoPLD activities. When examined at different pH from 4 to 11, mGDE7 showed the highest lysoPLD activity at pH 7.4–8.0 (data not shown).

3.2. Substrate specificities of recombinant GDE7 and GDE4

The sequence similarity of GDE7 to GDE4 encouraged us to examine whether both the proteins have similar substrate specificities or not. We then tested various *N*-acyl-lysoPEs and related molecules for the phosphodiesterase activities of these four enzymes. As shown in Fig. 5, these enzymes hydrolyzed all of *N*-[^{14}C]acyl-lysoPEs with different *N*-acyl species; *N*-oleoyl-lysoPE and *N*-arachidonoyl-lysoPE in addition to *N*-palmitoyl-lysoPE. The enzymes also hydrolyzed *N*-[^{14}C]palmitoyl-lysoPlsEt. GDE4 reacted with *N*-[^{14}C]palmitoyl-lysoPlsEt and *N*-[^{14}C]palmitoyl-lysoPE at similar rates, while the activity of GDE7 toward the former substrate was lower than that toward the latter substrate. As reported with mGDE7 and mGDE4 by Ohshima et al. [17] and with mGDE4 by us [16], 1-[^{14}C]palmitoyl-lysoPC was hydrolyzed by mGDE7 and mGDE4. The same reaction was also seen with hGDE7 and hGDE4. As compared with the reaction rates for *N*-[^{14}C]palmitoyl-lysoPE, those of hGDE7 and mGDE7 for 1-[^{14}C]palmitoyl-lysoPC were 1.2- and 2.3-folds higher, respectively, while those of hGDE4 and mGDE4 were only 9% and 10%, respectively. As for the reactivity with GP-NPE, a great difference was seen between GDE4 and GDE7. Although the membrane fraction of control cells showed a considerable [^{14}C]GP-NPE-hydrolyzing activity in the presence of $MgCl_2$, this reaction occurred at higher rates with the membrane fractions of the cells expressing hGDE4 and mGDE4 in accordance with our previous results shown by purified mGDE4 [16]. In contrast, hGDE7 and mGDE7 were almost inactive with [^{14}C]GP-NPE. The *N*-[^{14}C]palmitoyl-PE-hydrolyzing activities of both GDE7 and GDE4 were below the detection limit, indicating

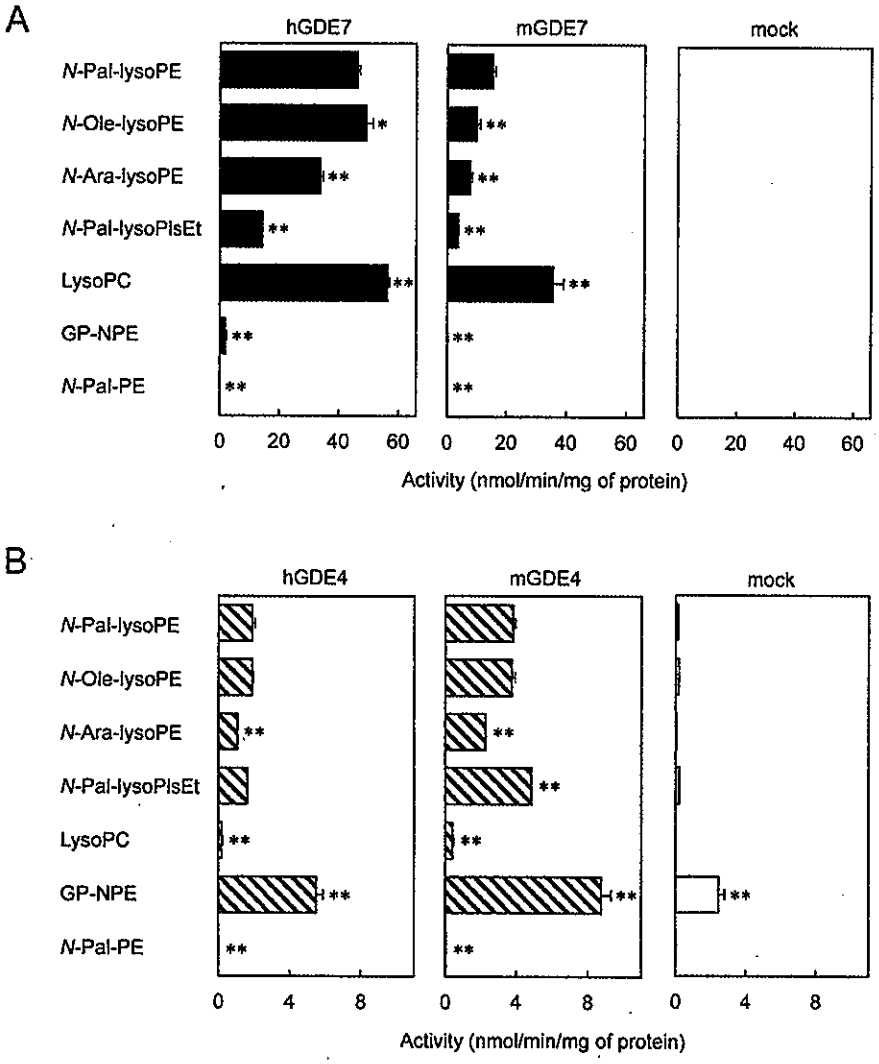

Fig. 5. Substrate specificities of hGDE7, mGDE7, hGDE4, and mGDE4. HEK293 cells overexpressing hGDE7 and mGDE7 (A) as well as hGDE4 and mGDE4 (B) and control cells (mock in A and B) were used to prepare membrane fractions. The membrane fractions (0.3–1 μg of protein in A and 1–2 μg of protein in B) were allowed to react with the indicated ^{14}C-labeled molecules at 25 μM in the presence of either 2 mM $CaCl_2$ (A) or 2 mM $MgCl_2$ (B). BHA at 10 μM was added to the reaction mixtures when the substrate was *N*-[^{14}C]arachidonoyl-lysoPE in order to protect arachidonic acid-containing molecules from autooxidation. The products were separated by TLC, and the calculated enzyme activities are expressed as mean values ± S.D. ($n = 3$). Ara, arachidonoyl; Ole, oleoyl; Pal, palmitoyl. *, $P < 0.05$; **, $P < 0.01$ compared with *N*-palmitoyl-lysoPE (ANOVA followed by Dunnett's test).

that neither enzyme has any NAPE-PLD-like activities. These results showed that GDE7 as well as GDE4 is a lysoPLD that is active with various lysophospholipids, including different species of *N*-acylated ethanolamine lysophospholipids.

3.3. Effects of divalent cations on the catalytic activity of GDE7

It was previously reported that the enzyme activities of GDE1 [15] and GDE4 [16] were enhanced by Mg^{2+} and inhibited by Ca^{2+}. We then examined the modulatory effects of 2 mM of various divalent cations on the *N*-[^{14}C]palmitoyl-lysoPE-hydrolyzing activities of hGDE7 (Fig. 6A) and hGDE4 (Fig. 6B). hGDE7 activity was as high as 28.0 nmol/min/mg of protein even in the absence of the exogenous divalent cations. The complete inhibition of the activity by 2 mM EDTA suggested that a certain endogenous divalent cation(s) contained in the membrane fraction potently stimulates GDE7 activity. Mg^{2+} reduced this activity to 54%, while Ca^{2+} enhanced it 1.5-fold. Fe^{2+} and Co^{2+} almost completely inhibited the activity. These results showed that Ca^{2+} rather than Mg^{2+} is a candidate divalent cation for stimulating GDE7 activity. In contrast, hGDE4 activity was increased by 10.0-fold in the presence of Mg^{2+}. Mn^{2+} also enhanced the activity of GDE4 by 8.9-fold. Other divalent cations tested, including Ca^{2+}, were inhibitory or ineffective. Since 2 mM EDTA completely abolished the GDE4 activity, the low activity detected in the absence of exogenous cations was

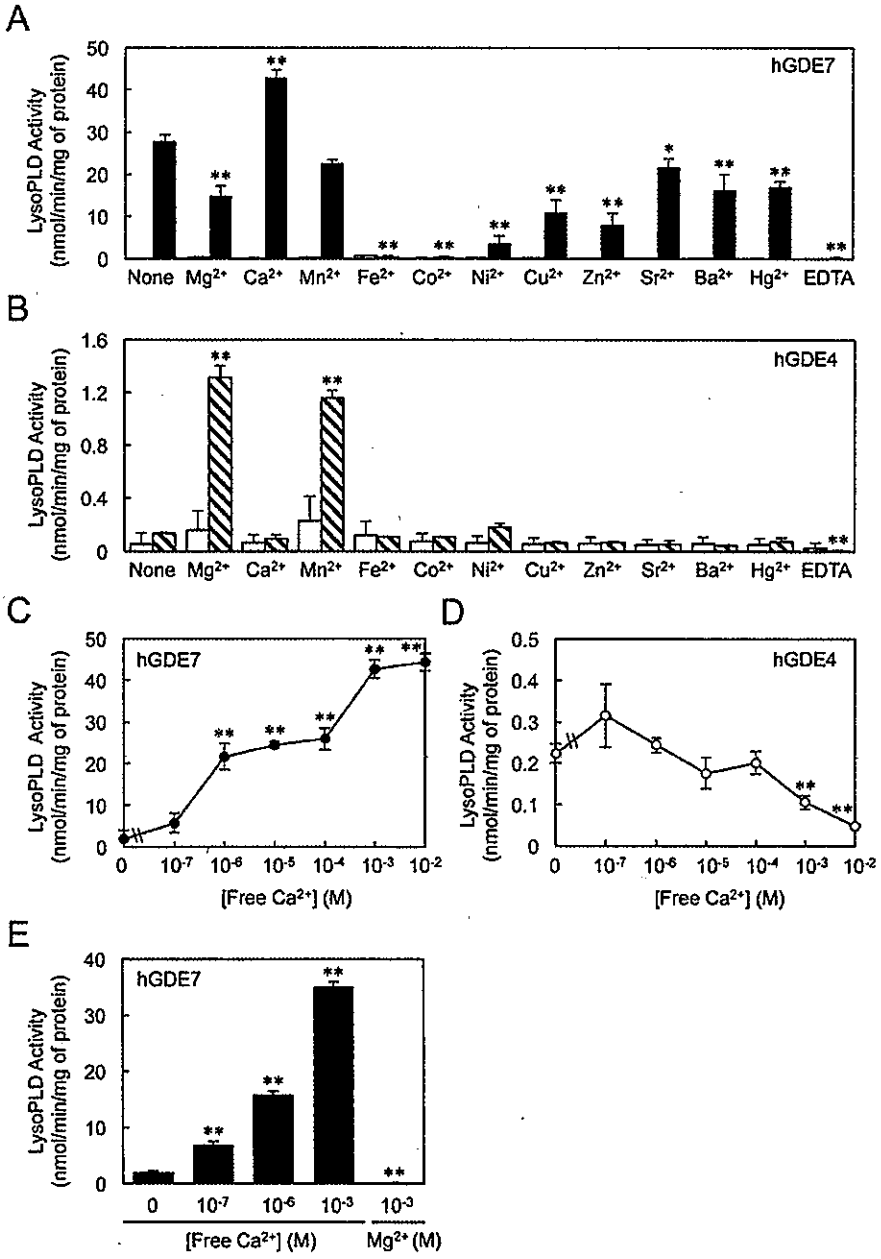

Fig. 6. Divalent cation requirements of GDE7 and GDE4. HEK293 cells overexpressing hGDE7 (closed columns and circles) or hGDE4 (hatched columns and open circles) and control cells (open columns) were used to prepare membrane fractions. The membrane fractions (0.3 μg (A, C, and E), 2 μg (B), and 5 μg (D) of protein) were allowed to react with *N*-[^{14}C]palmitoyl-lysoPE (A–D) or 1-[^{14}C]palmitoyl-lysoPC (E) at 25 μM. (A and B) the reactions were performed in the presence of the indicated divalent cations as 2 mM of chloride salt or 2 mM EDTA or in their absence (None). (C–E) the reactions were performed in the presence of the indicated concentrations of free Ca^{2+}, which were prepared by mixing 100 μM of EGTA and increasing concentrations of $CaCl_2$ [45]. In E, the reactions were also performed in the presence of 100 μM EGTA and 1 mM $MgCl_2$. The lysoPLD activities are expressed as mean values ± S.D. ($n = 3$). *, $P < 0.05$; **, $P < 0.01$ compared with the absence of divalent cations or EDTA (A and B) or the absence of Ca^{2+} (C–E) (ANOVA followed by Dunnett's test).

presumably attributed to divalent cations contained in the membrane fraction.

We thus examined the lysoPLD activities of hGDE7 and hGDE4 in the presence of increasing concentrations of free Ca^{2+} by using Ca^{2+}-EGTA buffer (Fig. 6C and D). Free Ca^{2+} dose-dependently stimulated the *N*-palmitoyl-lysoPE-hydrolyzing activity of GDE7, and the Ca^{2+} concentration required for a significant increase was as low as 1 μM. Contrary to GDE7, the activity of GDE4 was decreased depending on the increase in free Ca^{2+}. The stimulatory effect of Ca^{2+} on hGDE7 activity was also observed with the substrate 1-[^{14}C]palmitoyl-lysoPC (Fig. 6E). The significant increase was caused by 0.1 μM or higher concentrations of free Ca^{2+}. In the presence of 100 μM EGTA, 1 mM $MgCl_2$ showed no stimulatory effect. These results showed that the lysoPLD activity of GDE7 is stimulated by low concentrations of Ca^{2+}, and GDE7 was clearly distinguishable from GDE4 in this respect.

3.4. LC-MS/MS analyses of GDE7-expressing cells

We examined the effects of hGDE7 expression on endogenous levels of *N*-acylethanolamines and LPAs in HEK293 cells. LC-MS/MS analyses showed that most of *N*-acylethanolamine and LPA species were increased in hGDE7-overexpressing cells; however, the increased levels of several species were not statistically significant (Fig. 7). The total amounts of *N*-acylethanolamine and LPA species in the hGDE7-expressing cells were higher than those in control cells by 1.6- and 2.5-folds, respectively. Thus, GDE7 was suggested to function as an *N*-acylethanolamine-generating lysoPLD in intact cells.

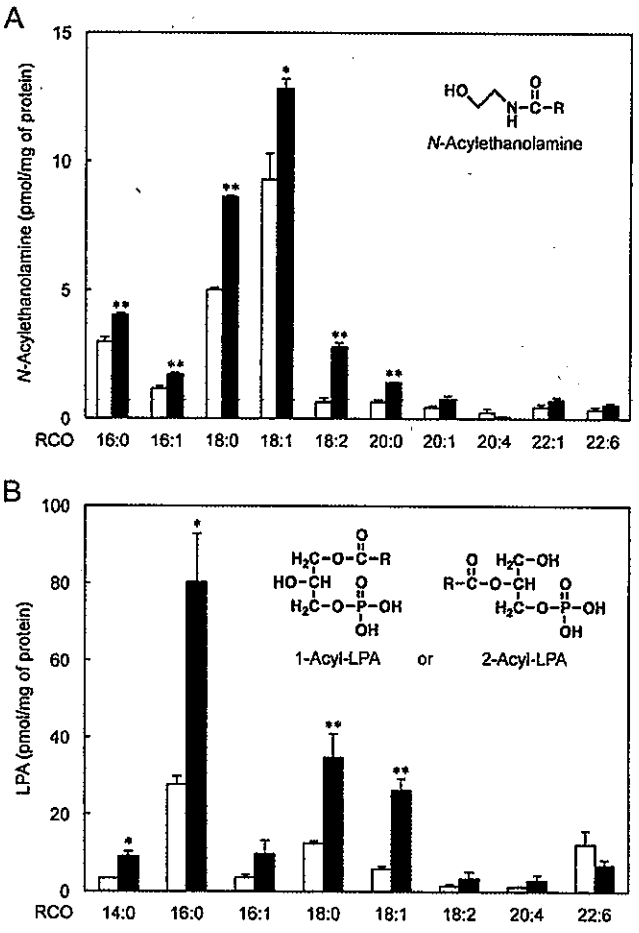

Fig. 7. Endogenous levels of *N*-acylethanolamines and LPAs in hGDE7-expressing HEK293 cells. HEK293 cells overexpressing hGDE7 (closed columns) or control cells (open columns) were analyzed for various molecular species of *N*-acylethanolamines (A) and LPAs (B) by LC-MS/MS. Bars represent mean values ± S.D. ($n = 3$). *, $P < 0.05$; **, $P < 0.01$ compared with control cells as analyzed by *t*-test.

3.5. Tissue distributions of hGDE7, hGDE4, and mGDE7

The tissue distributions of mRNAs for hGDE7, hGDE4, and mGDE7 were examined by RT-PCR (Fig. 8). Both of hGDE7 and mGDE7 mRNAs were widely distributed in various tissues. In particular, hGDE7 mRNA was the most abundant in the tissues of kidney and ovary, followed by placenta and prostate, while mGDE7 mRNA was predominantly expressed in stomach and kidney. On the other hand, hGDE4 mRNA was widely distributed with the most abundant expression in testis. The abundant expression corroborated our previous findings [16], which reported high expression levels of mGDE4 mRNA in testis. However, mGDE4 mRNA was also abundant in digestive tracts and brain [16]. We next selected kidney and brain of mouse as the tissues that highly expressed mGDE7 or hardly expressed it, respectively, and allowed the homogenates of these tissues to react with *N*-[^{14}C]palmitoyl-lysoPE and *N*-[^{14}C]palmitoyl-lysoPlsEt in the presence of 2 mM EGTA or EDTA or in their absence (Fig. 9). The formation of [^{14}C]palmitoylethanolamide from both the substrates was completely abolished by the addition of EDTA to both tissue homogenates, showing that endogenous lysoPLD(s) absolutely requires divalent cations. Interestingly, the effect of EGTA was different between brain and kidney. In brain, EGTA did not significantly decrease the lysoPLD activity toward *N*-[^{14}C]palmitoyl-lysoPE or *N*-[^{14}C]palmitoyl-lysoPlsEt, while in kidney EGTA decreased these activities to 36% and 53%, respectively. These results might be related to the different expression levels of GDE7 between these two tissues and suggested that the *N*-acylethanolamine-forming lysoPLD activity in mouse kidney is at least in part attributed to GDE7.

4. Discussion

Bioactive *N*-acylethanolamines are formed from NAPE through NAPE-PLD-dependent single-step and NAPE-PLD-independent multi-step pathways [9,10]. It was previously shown that members of the GDE family are involved in the latter pathway. Namely, mouse GDE1 showed a robust glycerophospho-*N*-acylethanolamine-hydrolyzing phosphodiesterase activity [13,15,16] and a weak *N*-acyl-lysoPlsEt-hydrolyzing lysoPLD activity [13,16] to produce *N*-acylethanolamines. We also showed that mGDE4 can hydrolyze *N*-acyl-lysoPlsEt and *N*-acyl-lysoPE as well as glycerophospho-*N*-acylethanolamine to *N*-acylethanolamine [16].

In the present study, we overexpressed recombinant proteins of human and mouse GDE7 as well as human and mouse GDE4, and compared their catalytic properties, including the substrate specificities. We first showed that the substrate specificity of hGDE4 is similar to that of mGDE4. Both GDE4s could hydrolyze various *N*-acylated lysophospholipids (*N*-palmitoyl-lysoPlsEt, *N*-palmitoyl-lysoPE, *N*-oleoyl-lysoPE, and *N*-arachidonoyl-lysoPE) and GP-NPE. Next, we showed for the first time that hGDE7 and mGDE7 also hydrolyze various *N*-acylated lysophospholipids to produce the corresponding *N*-acylethanolamines. The substrate specificity was found to be similar for both hGDE7 and mGDE7. When compared with GDE4, glycerophospho-*N*-acylethanolamine-hydrolyzing activity of GDE7 was much lower. Furthermore, while *N*-acyl-lysoPE-hydrolyzing activity of GDE4 was as potent as its *N*-acyl-lysoPlsEt-hydrolyzing activity, GDE7 preferred *N*-acyl-lysoPE to *N*-acyl-lysoPlsEt. Since *N*-acyl-lysoPE and *N*-acyl-lysoPlsEt have an ester and ether bond, respectively, at *sn*-1 position, the higher reactivity with *N*-acyl-lysoPE was consistent with previous observations that mGDE7 preferred 1-acyl-lysoPC to lyso-platelet activating factor (1-alkyl-lysoPC) while the substrate preference of mGDE4 was reverse [17]. Our LC-MS/MS data showed that the overexpression of hGDE7 resulted in increases in most molecular species of *N*-acylethanolamines as well as LPAs. This finding suggested

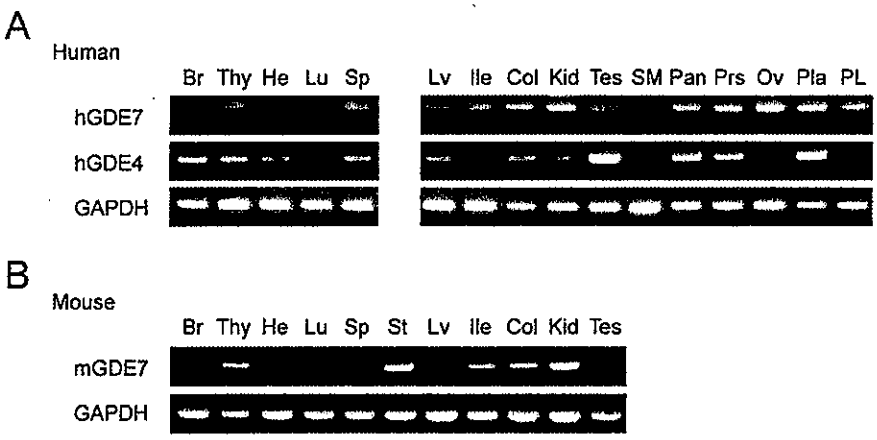

Fig. 8. Tissue distribution of mRNAs for hGDE7, hGDE4, and mGDE7. cDNAs from the indicated tissues of human (A) and mouse (B) were analyzed by PCR using primers specific for GDE7, GDE4, and GAPDH (a control). Br, brain; Thy, thymus; He, heart; Lu, lung; Sp, spleen; St, stomach; Lv, liver; Ile, ileum; Col, colon; Kid, kidney; Tes, testis; SM, skeletal muscle; Pan, pancreas; Prs, prostate; Ov, ovary; Pla, placenta; PL, peripheral leukocytes.

that GDE7 functions as an *N*-acylethanolamine-generating lysoPLD in intact cells.

Although both GDE7 and GDE4 had lysoPLD activities, the divalent cations required for their full activities were quite different from each other. Since EDTA abolished the activities of both enzymes, divalent cations were considered to be indispensable for their lysoPLD activities. Most interestingly, GDE7 was stimulated by Ca^{2+} in the micromolar range but was not activated by exogenous Mg^{2+}. In contrast, GDE4 was activated by Mg^{2+} but insensitive to Ca^{2+}, as was previously shown [16]. Since we used GDE7-expressing crude membrane fractions as enzyme sources, it was likely that they contained a low concentration of Ca^{2+} and therefore exhibited a considerable lysoPLD activity without adding exogenous Ca^{2+}. Thus, its Ca^{2+}-dependency became evident when Ca^{2+}-EGTA buffer was used. Furthermore, we could not rule out the possibility that other interacting protein(s) in the membrane fraction conferred the sensitivity to divalent cations, as reported with calmodulin and Ca^{2+}/calmodulin-dependent protein kinase II [28]. Both GDE7 and GDE4 were insensitive to Co^{2+} in sharp contrast to the potent activation of autotaxin, a well-characterized LPA-generating lysoPLD, by Co^{2+} [29,30]. The GDE family in mammals comprises seven members called GDE1–7 and most of them function as phosphodiesterases hydrolyzing glycerophosphodiesters (GDE1–5) and lysophospholipids (GDE4 and GDE7) [16,17,31,32]. Not only GDE4 but also GDE1 were reported to be stimulated by millimolar concentrations of Mg^{2+} and be insensitive to Ca^{2+} [15,33]. GDE5 was also active in the presence of 10 mM Mg^{2+} but not in the presence of 1 mM Ca^{2+} [34]. In contrast, 0.5–10 mM of Ca^{2+} stimulated GDE3 activity and Mg^{2+} was not required for its activity [35]. However, it was not investigated whether micromolar concentrations of Ca^{2+} activate GDE3.

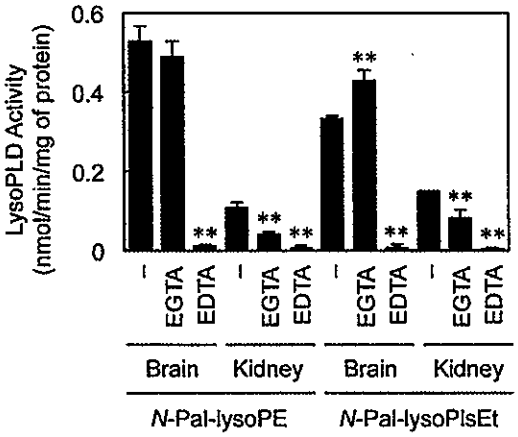

Fig. 9. The effects of EGTA and EDTA on lysoPLD activities of the tissue homogenates from mouse brain and kidney. The tissue homogenates (5 μg of protein) were allowed to react with 25 μM of *N*-[^{14}C]palmitoyl-lysoPE or *N*-[^{14}C]palmitoyl-lysoPlsEt in the presence of 2 mM of EGTA or EDTA or in their absence. The lysoPLD activities are expressed as mean values ± S.D. ($n = 3$). **, $P < 0.01$ compared with control (ANOVA followed by Dunnett's test).

All types of mammalian Ca^{2+}-dependent phospholipase C have EF-hand and C2 domains, known as Ca^{2+}-binding motifs [36–38]. However, GDE7 does not appear to have any EF-hand or C2 domains, and thus the molecular mechanism of the activation by Ca^{2+} remains unclear. GDE7 and GDE4 have two hydrophobic regions near the N- and C-termini. GlpQ and UgpQ are bacterial proteins structurally similar to GDE family members and have similar hydrophobic regions to those of GDE7 and GDE4 [31]. Interestingly, GlpQ was activated by millimolar concentrations of Ca^{2+} and inhibited by 4 mM of Mg^{2+} [39], while UgpQ was stimulated by 1–5 mM of Mg^{2+}, but not by 5 mM of Ca^{2+} [40]. These results suggested that a certain structural difference among the GDE family proteins determines the preference for Ca^{2+} or Mg^{2+}.

Autotaxin is an ecto/exo-enzyme generating LPA outside the cells [41,42]. In contrast, when overexpressed in HEK293 cells, recombinant GDE7 mostly resided in the membrane structures inside the cells (Fig. 3) and the release of GDE7 into culture medium was not observed (data not shown). GDE7-catalyzed LPA generation from lysoPC, the most common precursor of LPA, was also activated by micromolar concentrations of Ca^{2+}. These findings suggested that GDE7 produces LPA inside the cells in response to physiological stimuli, which increase intracellular Ca^{2+} levels.

As to the tissue distribution of mRNAs for GDE7 and GDE4, both mRNAs were expressed in various tissues of humans and mice. GDE7 mRNA was abundantly expressed in kidney of both humans and mice. Mouse stomach also highly expressed GDE7 mRNA, as was reported by Ohshima and others [17]. However, we could not examine its level in human stomach since the cDNA was unavailable. We and others previously reported the tissue distribution of GDE4 mRNA in mice, showing abundant expression in brain, stomach, small intestine, colon, and testis [16,17]. In the present study, we showed that GDE4 mRNA was highly expressed in brain and testis of humans.

These results suggested that GDE7 is involved in the NAPE-PLD-independent *N*-acylethanolamine formation but plays a different role from GDE4 in terms of substrate specificity, Ca^{2+}-dependency, and tissue distribution. In accordance with these findings, the decrease in the *N*-acylethanolamine-forming lysoPLD activity by EGTA was observed in kidney but not in brain, suggesting the partial contribution of Ca^{2+}-

dependent enzyme(s), such as GDE7, to the kidney activity. On the other hand, Mg^{2+}-dependent enzyme(s), including GDE4, may be dominant in mouse brain. Earlier, it was reported that the lysoPLD activity toward lysoPAF (1-*O*-alkyl-2-lyso-*sn*-glycero-3-phosphocholine) in the microsomal fractions from rabbit and rat kidney was stimulated by 5 mM of Ca^{2+} [43], while the lysoPLD in rat liver, rat brain, and mouse brain was stimulated by Mg^{2+} [13,43]. These Ca^{2+}- and Mg^{2+}-dependent lysoPLD activities may be at least partially attributed to GDE7 and GDE4, respectively.

In conclusion, we found that GDE7 as well as GDE4 acts as a lysoPLD to produce *N*-acylethanolamines and LPAs. Micromolar concentrations of Ca^{2+} stimulated the lysoPLD activity of GDE7 that makes this enzyme catalytically distinct from other members of the GDE family, such as GDE4. Further studies on GDE7 are required to elucidate its physiological contribution to the biosynthesis of *N*-acylethanolamines and LPAs.

Transparency document

The Transparency document associated with this article can be found, in online version.

Acknowledgments

This work was supported by Grants-in-Aid for Scientific Research (C) (K.T., grant number 26350894; T.U., 15K08278; N.U., 25460370 and 16K08589) from the Japan Society for the Promotion of Science, the Funds for Kagawa University Young Scientists 2015 (T.U.) and 2016 (K.T.), and grants from ONO Medical Research Foundation 2014 (K.T.) and the Japan Foundation for Applied Enzymology 2014 (N.U.). We are grateful to Katsuhisa Kawai, Yumi Tani, and Ami Yamada for technical assistance. We also acknowledge Divisions of Research Instrument and Equipment, Animal Experiment, and Radioisotope Research, Life Science Research Center, Kagawa University.

References

[1] H.H.O. Schmid, P.C. Schmid, V. Natarajan, *N*-acylated glycerophospholipids and their derivatives, Prog. Lipid Res. 29 (1990) 1–43.
[2] H.S. Hansen, B. Moesgaard, H.H. Hansen, G. Petersen, *N*-acylethanolamines and precursor phospholipids-relation to cell injury, Chem. Phys. Lipids 108 (2000) 135–150.
[3] W.A. Devane, L. Hanus, A. Breuer, R.G. Pertwee, L.A. Stevenson, G. Griffin, D. Gibson, A. Mandelbaum, A. Etinger, R. Mechoulam, Isolation and structure of a brain constituent that binds to the cannabinoid receptor, Science 258 (1992) 1946–1949.
[4] P.M. Zygmunt, J. Petersson, D.A. Andersson, H. Chuang, M. Sørgård, V. Di Marzo, D. Julius, E.D. Högestätt, Vanilloid receptors on sensory nerves mediate the vasodilator action of anandamide, Nature 400 (1999) 452–457.
[5] J. Lo Verme, J. Fu, G. Astarita, G. La Rana, R. Russo, A. Calignano, D. Piomelli, The nuclear receptor peroxisome proliferator-activated receptor-α mediates the anti-inflammatory actions of palmitoylethanolamide, Mol. Pharmacol. 67 (2005) 15–19.
[6] G. Mattace Raso, R. Russo, A. Calignano, R. Meli, Palmitoylethanolamide in CNS health and disease, Pharmacol. Res. 86 (2014) 32–41.
[7] J. Fu, S. Gaetani, F. Oveisi, J. Lo Verme, A. Serrano, F. Rodríguez De Fonseca, A. Rosengarth, H. Luecke, B. Di Giacomo, G. Tarzia, D. Piomelli, Oleylethanolamide regulates feeding and body weight through activation of the nuclear receptor PPAR-α, Nature 425 (2003) 90–93.
[8] D. Piomelli, A fatty gut feeling, Trends Endocrinol. Metab. 24 (2013) 332–341.
[9] N. Ueda, K. Tsuboi, T. Uyama, Metabolism of endocannabinoids and related *N*-acylethanolamines: canonical and alternative pathways, FEBS J. 280 (2013) 1874–1894.
[10] I.A.S. Rahman, K. Tsuboi, T. Uyama, N. Ueda, New players in the fatty acyl ethanolamide metabolism, Pharmacol. Res. 86 (2014) 1–10.
[11] Y. Okamoto, J. Morishita, K. Tsuboi, T. Tonai, N. Ueda, Molecular characterization of a phospholipase D generating anandamide and its congeners, J. Biol. Chem. 279 (2004) 5298–5305.
[12] G.M. Simon, B.F. Cravatt, Endocannabinoid biosynthesis proceeding through glycerophospho-*N*-acyl ethanolamine and a role for α/β-hydrolase 4 in this pathway, J. Biol. Chem. 281 (2006) 26465–26472.
[13] K. Tsuboi, Y. Okamoto, N. Ikematsu, M. Inoue, Y. Shimizu, T. Uyama, J. Wang, D.G. Deutsch, M.P. Burns, N.M. Ulloa, A. Tokumura, N. Ueda, Enzymatic formation of *N*-acylethanolamines from *N*-acylethanolamine plasmalogen through *N*-acylphosphatidylethanolamine-hydrolyzing phospholipase D-dependent and -independent pathways, Biochim. Biophys. Acta 1811 (2011) 565–577.
[14] K. Tsuboi, N. Ikematsu, T. Uyama, D.G. Deutsch, A. Tokumura, N. Ueda, Biosynthetic pathways of bioactive *N*-acylethanolamines in brain, CNS Neurol. Disord. Drug Targets 12 (2013) 7–16.
[15] G.M. Simon, B.F. Cravatt, Anandamide biosynthesis catalyzed by the phosphodiesterase GDE1 and detection of glycerophospho-*N*-acyl ethanolamine precursors in mouse brain, J. Biol. Chem. 283 (2008) 9341–9349.
[16] K. Tsuboi, Y. Okamoto, I.A.S. Rahman, T. Uyama, T. Inoue, A. Tokumura, N. Ueda, Glycerophosphodiesterase GDE4 as a novel lysophospholipase D: a possible involvement in bioactive *N*-acylethanolamine biosynthesis, Biochim. Biophys. Acta 1851 (2015) 537–548.
[17] N. Ohshima, T. Kudo, Y. Yamashita, S. Mariggiò, M. Araki, A. Honda, T. Nagano, C. Isaji, N. Kato, D. Corda, T. Izumi, N. Yanaka, New members of the mammalian glycerophosphodiester phosphodiesterase family: GDE4 and GDE7 produce lysophosphatidic acid by lysophospholipase D activity, J. Biol. Chem. 290 (2015) 4260–4271.
[18] P.C. Schmid, P.V. Reddy, V. Natarajan, H.H.O. Schmid, Metabolism of *N*-acylethanolamine phospholipids by a mammalian phosphodiesterase of the phospholipase D type, J. Biol. Chem. 258 (1983) 9302–9306.
[19] Y.-X. Sun, K. Tsuboi, Y. Okamoto, T. Tonai, M. Murakami, I. Kudo, N. Ueda, Biosynthesis of anandamide and *N*-palmitoylethanolamine by sequential actions of phospholipase A_2 and lysophospholipase D, Biochem. J. 380 (2004) 749–756.
[20] E.G. Bligh, W.J. Dyer, A rapid method of total lipid extraction and purification, Can. J. Biochem. Physiol. 37 (1959) 911–917.
[21] M.M. Bradford, A rapid and sensitive method for the quantitation of microgram quantities of protein utilizing the principle of protein-dye binding, Anal. Biochem. 72 (1976) 248–254.
[22] S. Kathuria, S. Gaetani, D. Fegley, F. Valiño, A. Duranti, A. Tontini, M. Mor, G. Tarzia, G. La Rana, A. Calignano, A. Giustino, M. Tattoli, M. Palmery, V. Cuomo, D. Piomelli, Modulation of anxiety through blockade of anandamide hydrolysis, Nat. Med. 9 (2003) 76–81.
[23] M. Mor, S. Rivara, A. Lodola, P.V. Plazzi, G. Tarzia, A. Duranti, A. Tontini, G. Piersanti, S. Kathuria, D. Piomelli, Cyclohexylcarbamic acid 3′- or 4′-substituted biphenyl-3-yl esters as fatty acid amide hydrolase inhibitors: synthesis, quantitative structure-activity relationships, and molecular modeling studies, J. Med. Chem. 47 (2004) 4998–5008.
[24] Y. Satoh, R. Ohkawa, K. Nakamura, K. Higashi, M. Kaneko, H. Yokota, J. Aoki, H. Arai, Y. Yuasa, Y. Yatomi, Lysophosphatidic acid protection against apoptosis in the human pre-B-cell line Nalm-6, Eur. J. Haematol. 78 (2007) 510–517.
[25] A. Tokumura, L.D. Carbone, Y. Yoshioka, J. Morishige, M. Kikuchi, A. Postlethwaite, M.A. Watsky, Elevated serum levels of arachidonoyl-lysophosphatidic acid and sphingosine 1-phosphate in systemic sclerosis, Int. J. Med. Sci. 6 (2009) 168–176.
[26] Y.-X. Sun, K. Tsuboi, L.-Y. Zhao, Y. Okamoto, D.M. Lambert, N. Ueda, Involvement of *N*-acylethanolamine-hydrolyzing acid amidase in the degradation of anandamide and other *N*-acylethanolamines in macrophages, Biochim. Biophys. Acta 1736 (2005) 211–220.
[27] P.A. Chang, H.B. Shao, D.X. Long, Q. Sun, Y.J. Wu, Isolation, characterization and molecular 3D model of human GDE4, a novel membrane protein containing glycerophosphodiester phosphodiesterase domain, Mol. Membr. Biol. 557 (2008) 557–566.
[28] M.M. Stratton, L.H. Chao, H. Schulman, J. Kuriyan, Structural studies on the regulation of Ca^{2+}/calmodulin dependent protein kinase II, Curr. Opin. Struct. Biol. 23 (2013) 292–301.
[29] A. Tokumura, E. Majima, Y. Kariya, K. Tominaga, K. Kogure, K. Yasuda, K. Fukuzawa, Identification of human plasma lysophospholipase D, a lysophosphatidic acid-producing enzyme, as autotaxin, a multifunctional phosphodiesterase, J. Biol. Chem. 277 (2002) 39436–39442.
[30] M. Umezu-Goto, Y. Kishi, A. Taira, K. Hama, N. Dohmae, K. Takio, T. Yamori, G.B. Mills, K. Inoue, J. Aoki, H. Arai, Autotaxin has lysophospholipase D activity leading to tumor cell growth and motility by lysophosphatidic acid production, J. Cell Biol. 158 (2002) 227–233.
[31] N. Yanaka, Mammalian glycerophosphodiester phosphodiesterases, Biosci. Biotechnol. Biochem. 71 (2007) 1811–1818.
[32] D. Corda, M.G. Mosca, N. Ohshima, L. Grauso, N. Yanaka, S. Mariggiò, The emerging physiological roles of the glycerophosphodiesterase family, FEBS J. 281 (2014) 998–1016.
[33] B. Zheng, C.P. Berrie, D. Corda, M.G. Farquhar, GDE1/MIR16 is a glycerophosphoinositol phosphodiesterase regulated by stimulation of G protein-coupled receptors, Proc. Natl. Acad. Sci. U. S. A. 100 (2003) 1745–1750.
[34] Y. Okazaki, N. Ohshima, I. Yoshizawa, Y. Kamei, S. Mariggiò, K. Okamoto, M. Maeda, Y. Nogusa, Y. Fujioka, T. Izumi, Y. Ogawa, Y. Shiro, M. Wada, N. Kato, D. Corda, N. Yanaka, A novel glycerophosphodiester phosphodiesterase, GDE5, controls skeletal muscle development via a non-enzymatic mechanism, J. Biol. Chem. 285 (2010) 27652–27663.
[35] D. Corda, T. Kudo, P. Zizza, C. Iurisci, E. Kawai, N. Kato, N. Yanaka, S. Mariggiò, The developmentally regulated osteoblast phosphodiesterase GDE3 is glycerophosphoinositol-specific and modulates cell growth, J. Biol. Chem. 284 (2009) 24848–24856.
[36] A.L. Drayer, M.E. Meima, M.W. Derks, R. Tuik, P.J. van Haastert, Mutation of an EF-hand Ca^{2+}-binding motif in phospholipase C of Dictyostelium discoideum: inhibition of activity but no effect on Ca^{2+}-dependence, Biochem. J. 311 (1995) 505–510.
[37] E.A. Nalefski, J.J. Falke, The C2 domain calcium-binding motif: structural and functional diversity, Protein Sci. 5 (1996) 2375–2390.
[38] Y. Nakamura, K. Fukami, Roles of phospholipase C isozymes in organogenesis and embryonic development, Physiology (Bethesda) 24 (2009) 332–341.
[39] T.J. Larson, M. Ehrmann, W. Boos, Periplasmic glycerophosphodiester phosphodiesterase of *Escherichia coli*, a new enzyme of the *glp* regulon, J. Biol. Chem. 258 (1983) 5428–5432.
[40] N. Ohshima, S. Yamashita, N. Takahashi, C. Kuroishi, Y. Shiro, K. Takio, *Escherichia coli* cytosolic glycerophosphodiester phosphodiesterase (UgpQ) requires Mg^{2+}, Co^{2+}, or Mn^{2+} for its enzyme activity, J. Bacteriol. 190 (2008) 1219–1223.

[41] J. Murata, H.Y. Lee, T. Clair, H.C. Krutzsch, A.A. Arestad, M.E. Sobel, L.A. Liotta, M.L. Stracke, cDNA cloning of the human tumor motility-stimulating protein, autotaxin, reveals a homology with phosphodiesterases, J. Biol. Chem. 269 (1994) 30479–30484.
[42] A. Giganti, M. Rodriguez, B. Fould, N. Moulharat, F. Cogé, P. Chomarat, J.-P. Galizzi, P. Valet, J.-S. Saulnier-Blache, J.A. Boutin, G. Ferry, Murine and human autotaxin α, β, and γ isoforms: gene organization, tissue distribution, and biochemical characterization, J. Biol. Chem. 283 (2008) 7776–7789.
[43] T. Kawasaki, F. Snyder, The metabolism of lyso-platelet-activating factor (1-O-alkyl-2-lyso-sn-glycero-3-phosphocholine) by a calcium-dependent lysophospholipase D in rabbit kidney medulla, Biochim. Biophys. Acta 920 (1987) 85–93.
[44] A. Krogh, B. Larsson, G. von Heijne, E.L. Sonnhammer, Predicting transmembrane protein topology with a hidden Markov model: application to complete genomes, J. Mol. Biol. 305 (2001) 567–580.
[45] T.J.M. Schoenmakers, G.J. Visser, G. Flik, A.P.R. Theuvenet, CHELATOR: an improved method for computing metal ion concentrations in physiological solutions, BioTechniques 12 (1992) 870–879.